

# Articles

## SAXS and USAXS Investigation on Nanometer-Scaled Precursors in Organic-Mediated Zeolite Crystallization from Gelating Systems

Peter-Paul E. A. de Moor,\* Theo P. M. Beelen, and Rutger A. van Santen

*Schuit Institute of Catalysis, Eindhoven University of Technology, P. O. Box 513,  
5600 MB Eindhoven, The Netherlands*

Katsuyuki Tsuji and Mark E. Davis

*Division of Chemistry and Chemical Engineering, California Institute of Technology,  
Pasadena, California 91125*

*Received March 25, 1998. Revised Manuscript Received October 14, 1998*

The formation of precursor particles in the crystallization of zeolites from gelating systems has been studied using X-ray scattering at small angles. The crystallization of Si–MFI using trimethylene-bis(*N*-hexyl, *N*-methyl-piperidinium) as the structure-directing agent shows the formation of two categories of precursors: gel particles and nanometer-scaled primary units. The size of the primary units for the crystallization of Si–MFI is found to be 2.8 nm both for gelating and nongelating systems using different structure-directing agents. Zeolites Si–BEA and Si–MTW have been prepared using the same organic (trimethylene-bis(*N*-benzyl, *N*-methyl-piperidinium)) at different concentrations. Primary units with a size of 2.6 nm are found to be present in the synthesis of Si–BEA, while their size is 1.5 nm in the synthesis mixture directing to Si–MTW. Our data suggest that the nanometer-scaled primary units are specific for the zeolite topology formed.

### Introduction

Microporous crystalline solids are industrially important materials applied in catalysis, ion exchange, and gas separation processes. Because of their well-defined (crystalline) morphology, there is a close relationship between their microscopical structure and macroscopic properties. This relationship has been a strong incentive for the synthesis of new materials with novel pore architectures and crystal compositions.<sup>1</sup> Many investigations have been carried out to understand the mechanisms in the conversion of amorphous reactants to microporous crystalline frameworks.

Traditionally, investigations on mechanisms in the crystallization of zeolites are often based upon observations of the products formed. Knowledge concerning the intermediates and their transformations is limited, mainly because of two experimental problems. First, the intermediates are often built from particles connected by relatively weak bonds, which makes them very fragile, and so only in situ experiments can give reliable results. Secondly, the dimensions of the intermediates are such (>1 nm) that most spectroscopic techniques

are not informative. Some problems can be circumvented using light-scattering techniques<sup>2–4</sup> and crystallizations from water clear solutions. Unfortunately, visible light scattering does not allow one to observe all precursor particles during the complete course of the crystallization process. Also, in most zeolite crystallizations a turbid gel phase is formed, for which visible light scattering cannot be informative.

Because thin layers of reaction mixtures are transparent to X-rays, we used X-ray scattering to probe samples irrespective of their consistency and appearance. The scattering of nano-sized entities by X-rays was observed at (very) small angles (<1°).

For the crystallization of Si–TPA–MFI from a clear solution, we were able to probe the formation and transformations of precursor particles during the whole course of the crystallization process.<sup>5,6</sup> We observed the formation of 2.8 nm sized primary units, as also reported

\* Author to whom correspondence should be addressed. Fax: +32 2 722 7280. E-mail: peterpaul.demoor@exxon.sprint.com.

(1) Lobo, R. F.; Zones, S. I.; Davis, M. E. *J. Inclusion Phenom. Mol. Recognit. Chem.* **1995**, *21*, 47.

(2) Twomey, T. A. M.; Mackay, M.; Kuipers, H. P. C. E.; Thompson, R. W. *Zeolites* **1994**, *14*, 162.

(3) Schoeman, B. J. In *Progress in zeolite and microporous materials*; Chon, H., Ihm, S.-K., Uh, Y. S., Eds.; Studies in Surface Science and Catalysis 105; Elsevier Science B. V.: New York, 1997; p 647.

(4) Schoeman, B. J.; Regev, O. *Zeolites* **1996**, *17*, 447.

(5) de Moor, P.-P. E. A.; Beelen, T. P. M.; Komanshek, B. U.; Diat, O.; van Santen, R. A. *J. Phys. Chem. B* **1997**, *101*, 11077.

(6) de Moor, P.-P. E. A.; Beelen, T. P. M.; Komanshek, B. U.; van Santen, R. A. *Microporous Mesoporous Mater.* **1998**, *21*, 263.

by Schoeman for fresh synthesis mixtures.<sup>3,4</sup> Additionally, we found a second population of amorphous precursor particles to be present (size  $\approx 10$  nm), depending on the alkalinity of the synthesis mixture. Using simultaneous small- and wide-angle X-ray scattering (SAXS/WAXS) we probed in situ on one sample the formation of the different precursor particles and their subsequent consumption in the nucleation and crystal growth process.

In this paper we report on a small-angle X-ray scattering study on the organic mediated crystallization of Si-MFI, Si-BEA, and Si-MTW from gelating systems, taking full advantage of the possibility to probe precursor particles in a heterogeneous gel phase. Using a combination of ultra-small-angle X-ray scattering (USAXS) and simultaneous SAXS/WAXS, we probed an extremely broad range of length scales (4 decades), allowing us to identify both the structure of the gel phase and the formation of nanometer-scaled primary units. The observed precursors in the crystallization of Si-MFI from a gel phase using trimethylene-bis(*N*-hexyl, *N*-methyl-piperidinium) as the structure-directing agent are compared with those formed in the synthesis of Si-TPA-MFI from a clear solution. Si-BEA and Si-MTW were synthesized using the same structure-directing agent at different concentrations, with the identification of correlations between the precursors present in the synthesis mixture and the crystalline structure formed as the main objective.

## Experimental Section

The crystallization of Si-MFI using trimethylene-bis(*N*-hexyl, *N*-methyl-piperidinium) as the structure-directing agent,<sup>7</sup> from a synthesis mixture with a molar composition of  $10\text{SiO}_2:3.0\text{R}(\text{OH})_2:0.5\text{NaOH}:350\text{H}_2\text{O}$ , was performed at 160 °C. In both the synthesis of Si-BEA at 150 °C and of Si-MTW at 160 °C, we used trimethylene-bis(*N*-benzyl, *N*-methyl-piperidinium) as the structure-directing agent. For Si-BEA the molar composition of the synthesis mixture was  $10\text{SiO}_2:1.5\text{R}(\text{OH})_2:0.5\text{NaOH}:350\text{H}_2\text{O}$ , and for Si-MTW it was  $10\text{SiO}_2:0.70\text{R}(\text{OH})_2:1.3\text{NaOH}:350\text{H}_2\text{O}$ . The preparation method of the synthesis mixtures was identical for all syntheses using bis-piperidinium compounds, and will be outlined here for the case of Si-MFI.

In a recovery flask 0.40 mmol of NaOH ( $=0.32$  g of 5 wt % solution in  $\text{H}_2\text{O}$ ) was added to 1.20 mmol of trimethylene-bis(*N*-hexyl, *N*-methyl-piperidinium) dihydroxide solution (1.486 g of 0.8074 mmol/g of solution in  $\text{H}_2\text{O}$ ) and shaken gently to get a homogeneous solution. Then 8 mmol of tetraethyl orthosilicate ( $=1.70$  g, Aldrich, 98 wt %) was added and the mixture was stirred for 3 h. The ethanol formed during the hydrolysis was removed using a vacuum evaporator at approximately 40–45 °C. Deionized water was added to obtain a molar ratio of  $\text{H}_2\text{O}/\text{SiO}_2 = 35$  (total weight synthesis mixture: 6.092 g). For Si-MFI, the fresh synthesis mixture was white cloudy, while it was an almost water clear solution in the case of Si-BEA and Si-MTW. After the mixture was heated to the reaction temperature, a heterogeneous gel phase was formed within a few minutes in all cases.

Synthesis of Si-TPA-MFI (TPA = tetrapropylammonium) from a completely water clear solution with a molar composition of  $10\text{SiO}_2:2.437\text{TPAOH}:1.695\text{NaOH}:113.9\text{H}_2\text{O}$  was performed at 125 °C as reported elsewhere.<sup>8</sup> In the preparation of the TPA-free solution (water glass), the molar composition was  $10\text{SiO}_2:4.132\text{NaOH}:113.9\text{H}_2\text{O}$ .

All measurements have been performed in situ in a special rotating (2 rpm), electrically heated sample cell. The sample thickness was 0.5 mm and mica windows (thickness 0.25  $\mu\text{m}$ ) were used. The scattering of water between the mica windows at the reaction temperature has been used as the background pattern.

The combined SAXS and WAXS experiments have been performed at station 8.2 of the Synchrotron Radiation Source at Daresbury Laboratory (United Kingdom),<sup>9</sup> using a camera length of 0.8 ( $0.4 < Q < 7$  nm<sup>-1</sup>) and 3.4 m ( $0.1 < Q < 2.5$  nm<sup>-1</sup>). The shape of the X-ray beam at station 8.2 was such that no desmearing of the SAXS data was needed. The USAXS experiments have been performed at the high-brilliance beamline ID2/BL4 of the European Synchrotron Radiation Facility in Grenoble (France) using a Bonse-Hart type of camera ( $0.001 < Q < 0.3$  nm<sup>-1</sup>). A detailed description of the used setup<sup>10</sup> and the data treatment and analysis<sup>5</sup> have been published previously. A configuration with two analyzer crystals has been used, so no desmearing was necessary. The resolution  $\Delta Q/Q$  of both the USAXS and SAXS setup was better than 0.02 over the whole  $Q$ -range. The  $Q$ -ranges obtained with the USAXS and SAXS showed sufficient overlap to allow an accurate merging of the patterns. Since no data was available on the absorbance of the samples, the recorded patterns could not be corrected to be an absolute scattering length density scale.

## Results

The results presented here are from both gelating and clear solution zeolite synthesis mixtures. The distinction is made on the appearance of the synthesis mixture: in a gelating system a heterogeneous, percolating  $\text{SiO}_2$  network is formed (i.e., a solid gel phase), while this is absent in the crystallization from a clear solution. In this paper we use the term gel particles for all amorphous precursors which are very large compared to the monomers they are built of ( $\geq 10$  nm). This means that the term gel particles can be used for precursor particles in a clear solution, where they do not form a percolating network but rather are present as dissolved particles.

**MFI.** The fresh liquid synthesis mixture had a white cloudy appearance. The scattering pattern from the fresh sample at room temperature (RT) (Figure 1A, line denoted RT), showed two weak "shoulders". The hump at approximately  $Q = 0.02$  nm<sup>-1</sup> was due to scattering by gel particles with a size of the order of 300 nm ( $d = 2\pi/Q$ ). The shoulder around  $Q = 2.5$  nm<sup>-1</sup> was due to scattering from nanometer-scaled precursors, which we denote primary units.

Within a few minutes of heating to a reaction temperature of 160 °C, a solid gel phase was formed. The scattering from the primary units now showed a maximum, as illustrated by the scattering pattern after 4 h (Figure 1A, I). This maximum points to the presence of interacting particles, such that preferred distances between the particles exist. This results in a maximum in the structure factor for this particle population, which gives a maximum in the observed scattering intensity.<sup>11,12</sup> The size of the particles was approximated to be 2.8–3.0 nm from the position of the maximum ( $d = 2\pi/Q$ ). At smaller scattering angles we now observed the

(9) Bras, W.; Derbyshire, G. E.; Ryan, A. J.; Mant, G. R.; Felton, A.; Lewis, R. A.; Hall, C. J.; Greaves, G. N. *Nucl. Instrum. Methods Phys. Res. Sect. A* **1993**, 326, 587.

(10) Diat, O.; Bösecke, P.; Lambard, J.; de Moor, P.-P. E. A. *J. Appl. Cryst.* **1997**, 30, 862.

(11) Bertram, W. *J. Appl. Cryst.* **1996**, 29, 682.

(12) Höhr, A.; Neumann, H. B.; Schmidt, P. W.; Pfeifer, P.; Avnir, D. *Phys. Rev. B* **1988**, 38, 1462.

(7) Tsuji, K.; Davis, M. E. *Microporous Mater.* **1997**, 11, 53.

(8) de Moor, P.-P. E. A.; Beelen, T. P. M.; van Santen, R. A. *Microporous Mater.* **1997**, 9, 117.

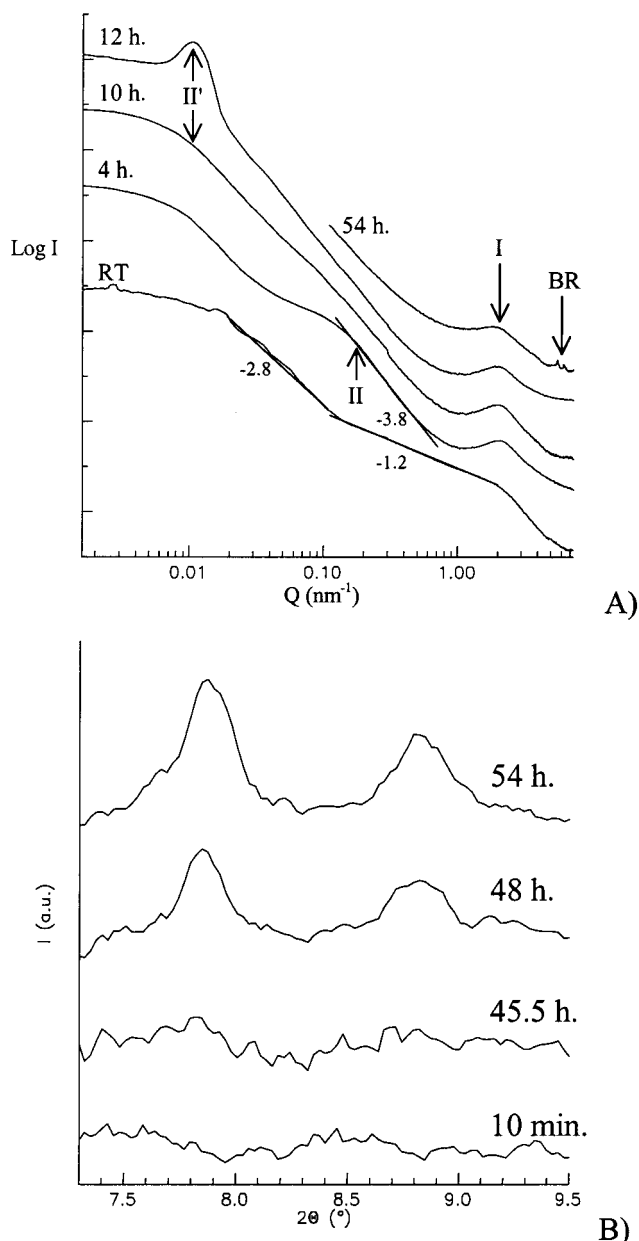


**Figure 1.** (A) Scattering patterns of a Si-MFI synthesis mixture using trimethylene-bis(*N*-hexyl, *N*-methyl-piperidinium) as the structure-directing agent. The annotations give the reaction time (RT refers to a fresh synthesis mixture before heating) and the slope of the linear fits. I = 2.8–3.0 nm sized primary units, II =  $\approx 40$  nm gel particles, II' =  $\approx 600$  nm gel particles, BR = Bragg reflections. For sake of clearness, the patterns have been shifted vertically. The scattering pattern for 54 h does not extend to very small angles since no USAXS is available for reaction times longer than 12 h. (B) The first two Bragg reflections as observed by the WAXS pattern after various reaction times.

scattering at two populations of gel particles. The smallest population ( $\approx 40$  nm, Figure 1A, II) gave rise to a linear region with a slope of  $-3.8 \pm 0.1$  in the log  $I$  versus log  $Q$  presentation of the scattering pattern, which corresponded to scattering at gel particles with a rather smooth surface<sup>13,14</sup> (a slope of  $-4$  would correspond to a perfectly smooth surface of spherical particles). The shoulder at  $Q \approx 0.01$  was probably the

scattering from the gel particles which were already present at room temperature, but which have grown promptly after heating to the order of 600 nm, resulting in a shift to smaller angles of the crossover to homogeneous scattering.

Two types of scattering patterns were recorded for reaction times longer than 6 h, depending on the part of the heterogeneous gel phase in the sample which was probed (Figure 1A, 10 and 12 h). The first type showed the scattering of two different precursor particles: the nanometer-scale primary units giving rise to a maximum at  $Q = 2.5 \text{ nm}^{-1}$  and gel structures with a size of  $\approx 600$  nm (shoulder at  $Q \approx 0.01 \text{ nm}^{-1}$  in Figure 1A, 10 h). The pattern after 12 h of heating showed two maxima: one at  $Q = 2.5 \text{ nm}^{-1}$ , which corresponds to the presence of the primary units, and a maximum at very small angles ( $Q \approx 0.01$ ). We can interpret this second maximum in the same way as the one due to the primary units: the scattering is due to strongly interacting particles which show preferred interparticle distances. Assuming a random orientation of the particles controlled by hard-sphere interactions, a maximum in the scattering curve will be observed for volume fractions of the spheres higher than 0.2. The clear maximum observed (Figure 1A, 12 h) can only be explained by the volume fraction of spheres higher than 0.4. Although the overall silica concentration in the synthesis mixture is not high enough to explain an overall volume fraction of gel spheres higher than 0.4, we believe that locally in the gel phase such concentrations can be present. This agrees with the observation by the eye that the gel phase is not homogeneous after heating more than 6 h. This is in agreement with fact that different patterns are observed depending on the part of the gel phase that is probed (compare in Figure 1A curves at 10 and 12 h). Bertram<sup>11</sup> found the position of the maximum in the scattering curve in the case of strongly interacting particles to correspond to the particle diameter ( $Q = 2\pi/d$ ). Here, the individual particles have a magnitude of approximately 600 nm. Since no crystallinity has been detected by the in situ WAXS at these reaction times (Figure 1B), the scattering entities with a size of 600 nm can be interpreted as being amorphous gel particles.

The onset of crystallization as determined from the appearance of Bragg reflections in the WAXS pattern was observed between 45.5 and 48 h of heating (Figure 1B). After a significant degree of crystallization took place (Figure 1B, 54 h), the maximum due to the scattering at the primary units was much more shallow than that before crystallization (Figure 1A, I). This suggests a decrease in the concentration of the primary units due to consumption in the crystallization process, but unfortunately accurate quantitative information cannot be obtained from these data.

For the crystallization of MFI from a water clear synthesis mixture, using TPA as a structure-directing agent, we found a correlation between the formation and consumption of precursor particles on one side and the crystallization behavior as determined from the Bragg reflections<sup>6</sup> on the other side. And 2.8 nm sized particles were observed from the onset of the reaction and amorphous  $\approx 10$  nm sized gel particles were formed prior to the onset of crystallization. As the crystallization

(13) Bale, H. D.; Schmidt, P. W. *Phys. Rev. Lett.* **1984**, *53*, 596.

(14) Martin, J. E.; Hurd, A. J. *J. Appl. Cryst.* **1987**, *20*, 61.



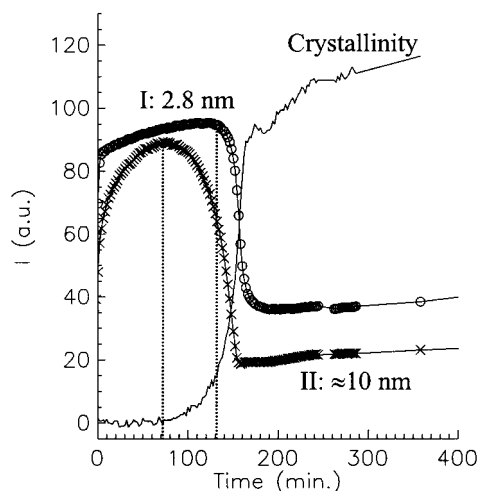


**Figure 2.** Scattering intensity from the different particle populations and the crystallization behavior as determined from the area of Bragg reflections for the crystallization of Si-TPA-MFI from a clear solution with Si/OH = 3.02 (taken from ref 6). I = 2.8 nm sized primary units. II =  $\approx 10$  nm gel particles.

starts, the consumption of the  $\approx 10$  nm sized gel particles is observed prior to the effective consumption of the 2.8 nm primary units (Figure 2). A similar behavior is observed in the gelating system using trimethylene-bis-(*N*-hexyl, *N*-methyl-piperidinium) as organic. Amorphous gel particles with a size of several tens of nanometers are formed after heating, while 2.8 nm sized primary units are present from the onset. The consumption of the gel particles (II in Figures 1A and 2) is observed prior to the consumption of the 2.8 nm sized particles. In the case of the clear solution synthesis, the consumption of the gel particles ( $\approx 10$  nm) agrees with the onset of crystallization, while their consumption in the heterogeneous gel synthesis is observed well before the onset of crystallization (Figure 1B).

The electron microscopy images show crystals with a broad size range from 80 to 600 nm. The particles do not show clear crystal faces, but were more or less cauliflower-shaped (Figure 3A). The rough surface of the crystals gives the impression that it is composed of 10–20 nm sized crystalline particles which mostly have the same orientation as the crystal. However, on close observation fringes can be observed which indicate the existence of several orientations at the surface (Figure 3B).

**BEA.** The scattering pattern of the fresh synthesis mixture of Si-BEA at room temperature is similar to that for the Si-MFI synthesis described above (Figure 4A). Since no USAXS data are available, the  $Q$ -range for the BEA and MTW cases is smaller than that for MFI. After heating the mixture to reaction temperature (150 °C), we again observed the formation of rather smooth (slope  $-3.8$ ) particles with a size in the order of several tens of nanometers. In this experiment we were able to follow their growth, by approximating their size from the  $Q$ -value where the linear fit levels off upon decreasing angle. The growth of the particles appears to be linear against the logarithm of the reaction time (Figure 4B). After 10 h of heating, the scattering of the gel particle population could not be observed any longer, because the size of the particles was larger than the

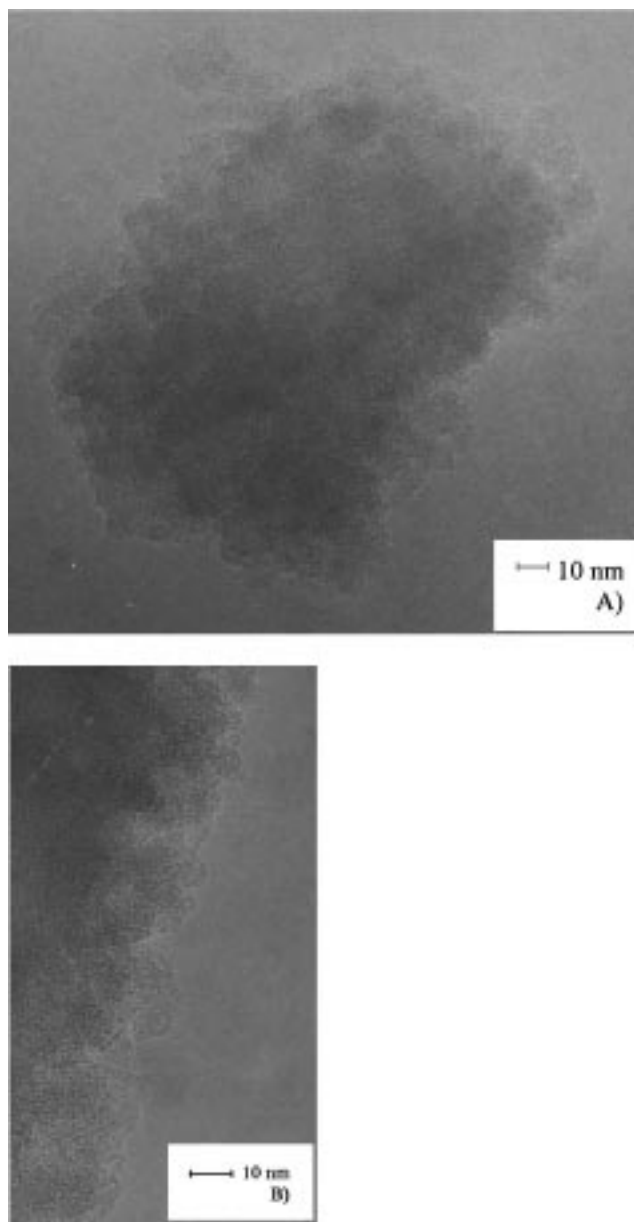


**Figure 3.** EM micrographs of Si-MFI prepared using trimethylene-bis(*N*-hexyl, *N*-methyl-piperidinium). (A) A typical crystal. (B) The surface morphology.

maximum  $d$ -spacing which could be probed. These particles are believed to be amorphous since crystalline particles of this size are expected to show peaks in the WAXS pattern, which is not observed. This does not exclude the presence of ordering in the silica which is typical for the BEA structure, but without the long-range ordering, as shown to be possible by Jacobs et al.<sup>15</sup>

As in the synthesis of Si-MFI, again the formation of nanometer-scale primary units was observed. Their size now is estimated to be 2.6 nm (Figure 4A, I). However, no pronounced maximum was observed for this synthesis, probably because of the lower concentration of the structure-directing agent for the synthesis of Si-BEA compared to that of the Si-MFI example. The first sign of crystallization of Si-BEA was observed after 20 h of heating (Figure 4C). Because the  $Q$ -range

(15) Jacobs, P. A.; Derouane, E. G.; Weitkamp, J. *Chem. Commun.* **1981**, 591–593.

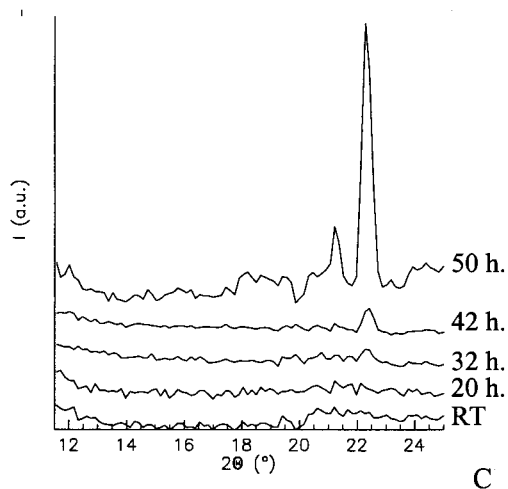
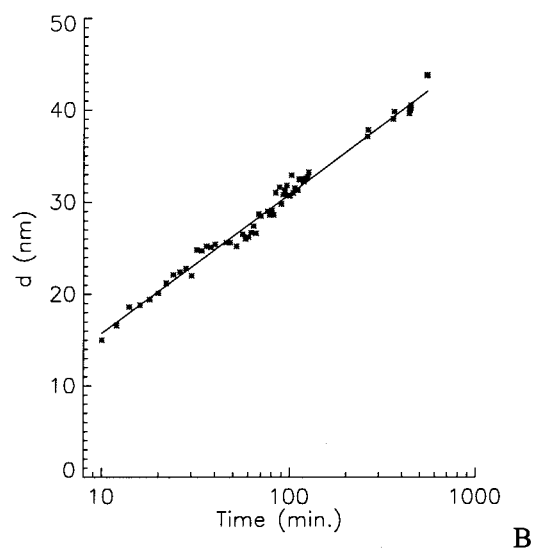
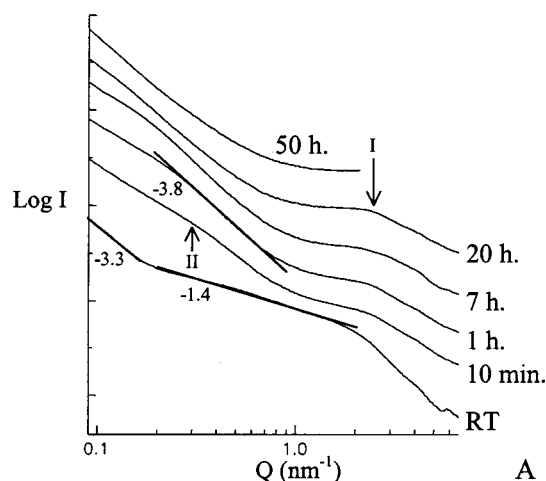


**Figure 4.** (A) Scattering patterns of a Si-BEA synthesis mixture using trimethylene-bis(*N*-benzyl, *N*-methyl-piperidinium) as the structure-directing agent. The annotations give the reaction time (RT refers to a fresh synthesis mixture before heating) and the slope of the linear fits.  $I = 2.6$  nm sized primary units, II = growing amorphous gel particles. Patterns have been shifted vertically. For a reaction time of 50 h only a restrict  $Q$ -range was available. (B) The size of the growing gel particles II as determined from the crossover where the scattering at the rather smooth particles (slope  $\approx -4$ ) levels off at a decreasing scattering angle. (C) The WAXS pattern for the crystallization of Si-BEA after various reaction times.

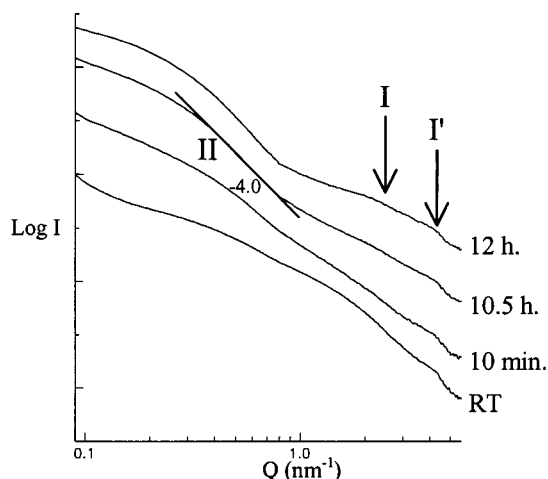


**Figure 5.** Scattering patterns of a Si-MTW synthesis mixture during the initial stage of the reaction (no data available after 12 h of heating).  $I = \approx 2.5\text{--}3.0$  nm sized primary units,  $I' = \approx 1.5$  nm primary units, II =  $\approx 15$  nm gel particles.

available was restricted for reaction times longer than 20 h, no correlation between the crystallization process and the consumption of precursor particles could be observed.

**MTW.** The scattering pattern for the synthesis mixture for Si-MTW at room temperature (Figure 5) shows resemblance to the corresponding patterns for the Si-MFI and Si-BEA syntheses. A slight indication of  $\approx 15$  nm particles is observed ( $Q \approx 0.4$  nm $^{-1}$ ). After the mixture was heated to a reaction temperature of 160 °C, the scattered intensity from these particles increased and a slope of  $-4$  in the  $\log I$  versus  $\log Q$  plots corresponded to the formation of smooth particles. These entities are believed to be amorphous since no sign of Bragg reflections is detected in the time range available. In contrast to the Si-BEA system, we do not find a growth of these particles until 12 h of heating. Again, we find the scattering at nanometer-scale precursors around  $Q \approx 2$  nm $^{-1}$ . The scattering at these entities is less pronounced than that for Si-BEA but seems to increase with an increasing reaction time. The lower intensity is probably related to a lower structure-directing agent concentration (less than half) for Si-MTW compared to the Si-BEA situation. The size of these particles is estimated to be 2.5–3.0 nm.

Additionally, a clearer shoulder is observed in the scattering pattern from the Si-MTW synthesis mixture at  $Q \approx 4.2$  nm $^{-1}$ , which can be explained by the presence of scattering entities of approximately 1.5 nm. Although the scattering at these particles is weak, they are believed to be present since the shallow shoulder is observed in all patterns measured for this system. On close observation, a sign of such a feature can also be observed in the scattering pattern of Si-BEA after 7 h of heating (Figure 4A). Unfortunately, no observations for the synthesis of Si-MTW for reaction times longer than 12 h are available (due to restricted beam time at the synchrotron), so the crystallization process could not be followed.

## Discussion

When comparing the scattering patterns observed for the syntheses of different zeolite types from a gel phase,

common features have been found. For the three synthesis mixtures prior to heating to reaction temperature the scattering patterns were similar, which is to be expected in view of the similar preparation methods. The wavy structure of the scattering patterns at room temperature (Figure 1A, RT, Figure 4A, RT, and although less clear, Figure 5, RT) can be explained as follows. The steep slope in the high- $Q$  region ( $>2\text{ nm}^{-1}$ ) is due to scattering at nanometer-scale primary particles. These primary particles are forming larger structures, aggregates, giving rise to the linear fit between  $Q = 0.2$  and  $2.0\text{ nm}^{-1}$ . The slope in this region is  $-1.2$  in the case of MFI (Figure 1A) and  $-1.4$  in the case of BEA (Figure 4A). These small slopes point to very low mass-fractal dimensions,<sup>16</sup> in other words, linear structures. This cannot be explained by a random aggregation process, which in the case of a diffusion-limited cluster-cluster aggregation process would result in a mass fractal dimension around 1.8. In the case of reaction-limited aggregation processes, higher mass fractal dimensions will be found, resulting in slopes in the log  $I$  versus log  $Q$  plot steeper than  $-2$ . The observed low fractal dimension can possibly be explained by a tip-tip-like aggregation process of anisotropic particles. If this indeed is the case, this would mean that the nanometer-scale primary units observed in the synthesis mixture at a very early stage do contain some anisotropy, possibly related to the topology of the final zeolite. The increasing intensity in the low- $Q$  region ( $<0.2\text{ nm}^{-1}$ ) can be explained by a second aggregation process, in which the aggregates of primary units serve as primary particles. The ordering of mass in this second type of aggregates is more dense, as evident from a steeper slope in the scattering pattern:  $-2.8$  for MFI (Figure 1A), and approximately  $-3.3$  for BEA (Figure 4A).

Another possible explanation could be that the wavy pattern is due to the form factor of rather monodisperse gel spheres. During heating the gel particles grow, resulting in the observed shift of the waves to lower  $Q$ -values (see Figure 1A, going from RT to 4 h). However, fitting the calculated scattering pattern of a polydisperse system of spheres to the experimental curves showed that the positions of the maxima and minima do not agree (for detail concerning the fitting procedure, see our previous report in ref 5). Therefore, it is believed that the wavy pattern should not be explained as being due to the form factor oscillations of scattering spheres, but rather to scattering at aggregates formed by two successive aggregation steps as explained in the previous paragraph.

After the mixture was heated to reaction temperature, the formation of two categories of precursor particles has been observed: gel particles (between 10 and 600 nm) and primary units (order of a few nm). For the Si-MFI synthesis we have shown that two types of gel particles are present, sized 40 and 600 nm, respectively. A population of particles with a size of several tens of nanometers was present in all three gelating systems, and consist of entities with rather smooth surfaces as illustrated by a slope near  $-4$  in the log  $I$  versus log  $Q$  plot (Figures 1A, 4A, and 5). From the SAXS patterns

for the Si-BEA synthesis mixture we could deduce that these particles grow in time (Figure 4B). In the clear solution synthesis of Si-TPA-MFI, we also observed the formation of gel particles ( $\approx 10\text{ nm}$ ), from which the scattering intensity decreased during the crystallization process (Figure 2). This decrease in the scattering intensity points to the consumption of the gel particles and coincides with the onset of crystallization. This can be explained by their transformation into nuclei, and their dissolution to smaller species which are consumed in the crystal growth process. For Si-MFI from a heterogeneous gel, this gel particle population was not observed for reaction times longer than 10 h (Figure 1A), which is significantly before the onset of crystallization as determined from the formation of Bragg reflections. Therefore, a different explanation for the disappearance of their scattering is more probable. It is unlikely in this stage of the reaction (well before crystallization) that the gel particles disappear by dissolution. Our data suggest that the particles become indistinguishable from the much larger (600 nm) gel particles. Probably the 40 nm particles are already part of the 600 nm gel structures, and transform in the aging process. After fusing, finally only the larger structure can be recognized. In this situation there is not a consumption of the particles, but the process can be described better by a transformation, the 40 nm particles becoming indistinguishable as separate entities. Therefore, similar processes in both the gel phase and clear solution synthesis can be expected, like the transformation of the gel particles to nuclei and dissolution to smaller entities which are consumed in the crystal growth.

The second category of precursor particles, nanometer-scaled primary units, appears to be present in all three systems studied here. For Si-MFI, these primary units have the same size ( $\approx 2.8\text{ nm}$ ) in both the synthesis from a heterogeneous gel and from a clear solution, using trimethylene-bis(*N*-hexyl, *N*-methyl-piperidinium) and TPA<sup>6</sup> respectively as the structure-directing agent (Figure 6). This suggests that the size of the primary units is determined by the properties of the structure-directing agent other than its tertiary size. Also, in both synthesis mixtures we observe a decrease in the scattering intensity from the primary units during the crystallization (Figure 1A, 54 h and Figure 2). This points to the consumption of these nanometer-scale precursors in the crystallization process, irrespective of the consistency of the synthesis mixture.

The scattering from the primary units is less pronounced for Si-BEA and Si-MTW than for Si-MFI, probably due to the concentration of the structure-directing agent in the synthesis mixture: the lower the concentration of the organic, the less pronounced the scattering pattern of the nanometer-scaled primary units (Figure 6). The scattering patterns for Si-MTW suggest that two different populations of primary units are present, with an estimated size of 3 nm and 1.5 nm ( $I$  and  $I'$ , respectively, in Figure 5). The scattering at the 1.5 nm sized particles has not been observed in the case of Si-MFI (Figure 1A) and Si-TPA-MFI,<sup>6</sup> and only a weak indication is observed for the Si-BEA synthesis (Figure 4A, 7 h,  $Q \approx 4.2\text{ nm}^{-1}$ ). This suggests that these 1.5 nm particles are specific for the crystallization of Si-MTW.

(16) Jullien, R.; Botet, R. *Aggregation and fractal aggregates*; World Scientific, 1987.

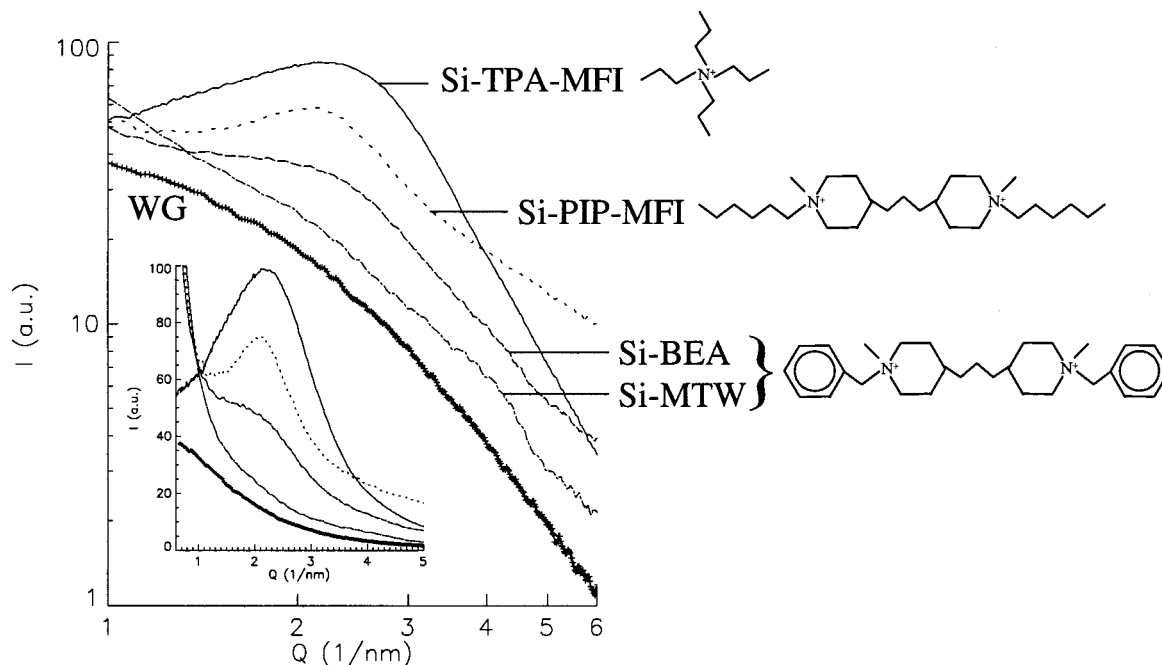


**Figure 6.** Log  $I$  vs log  $Q$  representation of the SAXS patterns for different zeolite synthesis mixtures after heating to the reaction temperature, but well before the onset of crystallization. The pattern annotated with WG corresponds to a solution without any organic (water glass). The inset shows the same plot with linear axes.

A similar change in the crystalline structure formed using one organic has been observed for the crystallization of Si-MFI and Si-ZSM-48 using 1,6-hexanediamine.<sup>17,18</sup> From synthesis mixtures with the same composition, the intersecting 10-ring pore structure MFI is formed at relatively low temperatures (120 °C), while the linear 10-ring pore structure of Si-ZSM-48 is formed at higher temperatures (150 °C). Burkett and Davis<sup>18</sup> used  $^1\text{H}$ - $^{29}\text{Si}$  cross polarization NMR to probe the organic-inorganic interactions at early stages of the zeolite synthesis. They found the intermolecular cross polarization at an early stage in zeolite synthesis (X-ray amorphous synthesis mixture) to be much more efficient for the synthesis of Si-MFI than for Si-ZSM-48. This suggests the closer contact between organic and inorganic components to be present in the Si-MFI. On the basis of these results, and on the observation that Si-ZSM-48 can be synthesized using a variety of organics, Burkett and Davis concluded that 1,6-hexanediamine acts as a real structure-directing agent in the Si-MFI synthesis, and as a pore-filling agent for Si-ZSM-48. Both in this paper and in a previous publication<sup>7</sup> we find the crystallization of the intersecting 12-ring pore architecture BEA to dominate at relatively low temperatures (135–150 °C), while the linear 12-ring pore zeolite MTW more readily crystallizes at higher temperatures (150–165 °C). Again, we suspect this change to be due to a transition from true structure directing (BEA) to pore filling (MTW), which might be related to the conformation of the organic.<sup>7</sup> Thus, the observation of the additional 1.5 nm primary units for MTW compared to BEA could be related to different organic-inorganic interactions, and therefore different types of crystallization mechanisms.

The primary units observed here probably play an important role in the nucleation and crystallization

mechanism. For the crystallization of Si-MFI from a completely clear solution, using TPA as a structure-directing agent and silicic acid as silica source, we recently clearly identified primary units in the synthesis mixtures. Now, for the first time, we show that in a completely different synthesis mixture (a bis-piperidinium as the structure-directing agent and TEOS as the silica source), also primary units with the same size are present besides large gel structures (compare Si-TPA-MFI and Si-PIP-MFI in Figure 6). As a control experiment we prepared a solution from which TPA was omitted (water glass), and no formation of primary units has been observed. The size of the primary units scales well with the unit cell dimension of the zeolite being formed (MFI:  $2.0 \times 2.0 \times 1.3$  nm), and Schoeman<sup>3</sup> reports that they do contain TPA. Burkett and Davis<sup>19,20</sup> studied the interaction between template molecules (TPA) and silica species prior to the onset of crystallization. They trapped the composite organic/inorganic species by silylation methods and showed they contained an IR band at  $560\text{ cm}^{-1}$ , which is indicative of organization of the silicate into rings of the type in the MFI crystals. These results could not be rationalized in light of single TPA molecules surrounded by silicate species. The observation of the 2.8 nm sized primary units enables understanding of previous results since their size allows several template molecules and silica to interact and form organization specific for the zeolite topology. Therefore, we believe that the primary units observed contain template molecules and play an important, and most probably essential, role in the zeolite nucleation and crystal growth process.

Resemblances have been observed in the formation of precursors in the crystallization of all-silica zeolites from gelling systems as reported here, and as reported earlier from a clear synthesis mixture.<sup>6</sup> In all cases

(17) Franklin, K. R.; Lowe, B. M. *Zeolites* **1988**, 8, 495.

(18) Burkett, S. L.; Davis, M. E. *Chem. Mater.* **1995**, 7, 1453.

(19) Burkett, S. L.; Davis, M. E. *J. Phys. Chem.* **1994**, 98, 4647.

(20) Burkett, S. L.; Davis, M. E. *Chem. Mater.* **1995**, 7, 920.



nanometer-scaled primary units were found to be present prior to heating. At the reaction temperature, the formation of amorphous gel particles in the size range of several tens of nanometers was observed. The agreement between the precursor particles formed in both systems for crystallizing Si-MFI and the consumption of the primary units suggests there is a common assembly process irrespective of the formation of a heterogeneous gel phase.

### Conclusions

Using in situ X-ray scattering techniques we were able to probe the precursor particles in gelating synthesis mixtures for the organic-mediated crystallization of zeolites Si-MFI, Si-BEA, and Si-MTW. Two categories of precursors have been observed: gel particles and nanometer-scaled primary units.

Two types of gel particles were observed: one with a size of several tens of nanometers which was shown to grow with time for the synthesis of Si-BEA. The second type of gel particles was much larger ( $\approx 600$  nm for Si-MFI). A comparison to the results obtained from Si-TPA-MFI crystallizations from a clear solution, in which also gel particles ( $\approx 10$  nm) are formed, shows that the formation of such large gel structures or a heterogeneous gel phase is no requisite for zeolite nucleation and growth.

We showed that nanometer-scaled primary units are present in gelating synthesis mixtures. For Si-MFI these particles have the same size (2.8 nm) as that observed in the synthesis from a completely clear solution. This size allows us to understand the observation of an IR band at  $560\text{ cm}^{-1}$  prior to the formation of

long-range order: several template molecules can interact with silicate species in one particle to form an order of the type as that observed in the final crystal. The size of the primary units is not determined by the size of the organic structure-directing agent used, but probably by its ability to order a silica shell around itself.

Synthesis mixtures containing trimethylene-bis(*N*-benzyl, *N*-methyl-piperidinium) can crystallize to Si-BEA and Si-MTW, depending on the synthesis conditions. And 1.5 nm sized primary units are exclusively observed in the synthesis mixture of Si-MTW. These results, and a comparison to the synthesis of Si-MFI or Si-ZSM-48 (using 1,6-hexanediamine) dependent on the temperature, suggests that the organic acts as a real structure-directing agent in the synthesis of Si-BEA, while it functions as a pore-filling agent for Si-MTW.

**Acknowledgment.** The SAXS/WAXS experiments were performed by an EPSRC grant at the Daresbury Synchrotron Radiation Source, where good help was provided by Dr. B. U. Komanschek. USAXS measurements were performed at the European Synchrotron Radiation Facility under Grants SC-138 and SC-202. We thank Dr. O. Diat for installing and perfectly aligning the Bonse-Hart setup. Dr. P. J. Kooyman of the National Centre for High Resolution Electron Microscopy, Delft University of Technology, Delft, The Netherlands, is acknowledged for performing the electron microscopy investigations. The work at CalTech was partially supported by the Chevron Research and Technology Company.

CM9807079